Available online at www.sciencedirect.com
ScienceDirect
Journal of the European Ceramic Society 30 (2010) 1469–1476
www.elsevier.com/locate/jeurceramsoc

# Effects of $BaO–SiO_2$ glass particle size on the microstructures and dielectric properties of Mn-doped $Ba(Ti, Zr)O_3$ ceramics

Ting-An Jain [a,*], Kuan-Zong Fung [a], Shawn Hsiao [b], Johnny Chan [b]

[a] *Department of Materials Science and Engineering, National Cheng Kung University, No.1, University Road, Tainan 701, Taiwan, ROC*
[b] *Darfon Electronics Corp., 21 Industry II Road, Annan, Tainan 709, Taiwan, ROC*

Received 29 July 2009; received in revised form 23 October 2009; accepted 4 November 2009
Available online 4 December 2009

**Abstract**

The sintering behavior, microstructures and dielectric properties of Mn-doped $Ba(Ti, Zr)O_3$ (BTZ) ceramics with different particle sizes of $BaO–SiO_2$ glass (D50 ranging between 185 and 1200 nm) were investigated. From the metallographic observation, adding finer glass frit revealed more homogeneous compositional distribution. It was found that better spreading of the glass phase could be achieved by adding finer glass particles that could penetrate the BTZ ceramic interface more easily, thus enhancing the grain growth. The extent of the incorporation between glass and ceramic increased with smaller glass particles, and the Curie temperature was altered accordingly. Microstructural evaluation conducted by using X-ray diffraction (XRD) and transmission electron microscopy (TEM) with an energy-dispersive X-ray spectrometer (EDS) indicated the glass particle size has a dramatic influence on the sintering behavior and microstructure of Mn-doped BTZ ceramics. The relationship between microstructures and dielectric properties was also discussed in this study.


*Keywords:* Grain growth; Electron microscopy; Dielectric properties; $BaTiO_3$; Capacitors

## 1. Introduction

Multilayer ceramic capacitors (MLCCs) are one of the most important electronic components because of their economical volumetric efficiency for capacitance and high reliability. High performance MLCCs need to possess a high intrinsic dielectric constant ($K$) and thinner dielectric layers as the market drives electronic devices towards ever-greater miniaturization and multifunctionality. To obtain high volumetric efficiency for electronic components, the technical trend is towards reduced dielectric thickness and increased stacking of electrode layers.[1,2] However, the applied electric field rises significantly with a reduction in dielectric thickness. The degradation of the isolation resistance (IR) of dielectrics at a high electric field depends strongly on the related microstructures, such as the grain size of the ceramics.[3] Dielectric materials with a smaller grain size are essential for Ni-MLCCs with thinner dielectric layers that can retain sufficient reliability, since the grain boundary characteristics play an important role in the resistance degradation behavior.[4] However, the dielectric constant of barium titanate based ceramic materials is greatly dependent on the grain size. Specifically, a higher dielectric constant obtained with coarser grains can achieve higher capacitance.[5,6] Therefore, precise grain size control to obtain compact ceramic materials with a finer and more homogeneous grain size is very important with regard to producing thinner dielectric layers with the desired capacitance and reliability.

$Ba(Ti, Zr)O_3$ (BTZ) is widely used as a dielectric ceramic material for multilayer ceramic capacitors because of its high dielectric constant.[7,8] The addition of acceptors, such as MnO and $Cr_2O_3$, has been developed to achieve non-reducible dielectrics.[1,9,10] It is considered that conduction electrons are trapped by the acceptors, so that the decrease in insulating resistance is suppressed. Sintering of BTZ at temperatures of 1350–1450 °C is required for the proper densification of powder pallets.[11] However, such a high sintering temperature is harmful for BTZ that is co-fired with inner electrodes, such as nickel or copper. The shrinkage mismatch between BTZ ceramics and metallic electrodes rises significantly with increasing sintering temperature, and this will lead to fractures in MLCC chips. This problem is exacerbated when the electrode layer is increased to gain higher capacitance with thinner dielectric

* Corresponding author. Tel.: +886 62757575x62969; fax: +886 62380208.
*E-mail address:* tajain@xuite.net (T.-A. Jain).

0955-2219/$ – see front matter © 2009 Elsevier Ltd. All rights reserved.
doi:10.1016/j.jeurceramsoc.2009.11.006

layers. The co-firing temperature must then be lowered to reduce the shrinkage mismatch between BTZ ceramics and the nickel electrode. Moreover, MLCC chips composed with poorly sinterable dielectric materials exhibit reduced IR and humidity resistance. However, the addition of glass to BTZ ceramics is an effective method which promotes densification by enabling liquid phase sintering at low temperatures. To date, various kinds of materials have been used, including barium oxide, alumina oxide, and silicon oxide, to lower the sintering temperature.[12–21] Although the $BaO–SiO_2$ glass system has been widely used as a liquid sintering aid for BTZ ceramics, the addition of glass may also introduce several undesirable effects, such as a decrease in the dielectric constant and the formation of pores and a secondary phase, which may lead to the degradation of dielectric properties. Therefore, how to obtain complete sinterability and high permittivity ceramics with the minimum addition of glass frit, thus preventing the undesirable side effects, is a topic of some importance.

It has been reported that the grain growth of BTZ-series ceramics is significantly influenced by the presence of the liquid phase.[8] Specifically, grain growth is enhanced by capillary, rearrangement and solution reprecipitation of the liquid phase at lower sintering temperatures. In contrast, grain growth may be restrained by liquid penetration on the grain boundaries at higher temperatures. The addition of glass frit also has significant effects on the dielectric and piezoelectric properties of BTZ ceramics. Wang et al.[12] studied the influence of glass composition on the densification and dielectric properties of $BaTiO_3$ ceramics. They found that the glass not only acts as a fluxing agent for liquid phase sintering, but also as a modifier of the dielectric properties when the glass component is incorporated into the $Ba(Ti, Zr)O_3$ lattices. The extent of incorporation and the distribution of the incorporated atoms may alter the Curie temperature, the sharpness of the phase transition and the *K* value of the ceramics. Moreover, the homogeneous distribution of glass in the grain boundaries is very important, since small amounts of the inhomogeneous liquid phases give rise to the abnormal grain growth and the segregation of glass in the grain boundaries has been found to reduce the dielectric properties.[13] The distribution of additives in BTZ powders is critical, since the additives are coarse and the amount is very small. In addition, the uniform distribution of additives is more difficult when the BT or BTZ particle size becomes smaller. To obtain suitable dielectric ceramics for MLCCs, the most important step is to control the homogeneity of glass additives in order to achieve a high level of densification with limited grain growth. This will minimize the amount of glass addition required, and prevent the formation of low dielectric secondary phases and the consequent variation in dielectric properties. Unfortunately, the influence of glass particle size on homogenization, microstructure and dielectric properties is not yet fully understood. In the present investigation, the sintering behavior, microstructures and dielectric properties of Mn-doped $Ba(Ti, Zr)O_3$ (BTZ) ceramics with various particle sizes of $BaO–SiO_2$ glass were thus measured to investigate the effect of glass homogenization on such ceramics.

## 2. Experimental procedure

The experiment consists of three parts: preparation of glass frit with different particle sizes, sample preparation, and evaluation of the dielectric characteristics.

### 2.1. Preparation of glass frit with different particle sizes

The $BaO–SiO_2$ glass system was used in the study. Calculated amounts of reagent-grade chemicals BaO, $SiO_2$ were weighed, mixed and melted in a platinum crucible in an air atmosphere at 1350 °C for 2 h. The molten glasses were quenched and then crushed in an agate bowl. A professional attrition mill (Model: 01-Lab Attritor, Union Process Inc., USA) with a cooling water jacket was used for glass size reduction. The grinding chamber and rotor were coated with urethane and manufactured zirconia ceramic, respectively to prevent metal contamination. The total capacity of the cylindrical chamber was 750 $cm^3$, and 380 $cm^3$ of media was mixed using yttria stabilized zirconia (YSZ) balls with diameters of 0.3 and 1 mm. The working capacity was 250 $cm^3$, and 100 g of BTZ powder was used per milling batch. The size of the particles was controlled by attrition milling for different times to get four different size distributions. To estimate the size distribution, the powders were sampled and characterized regularly by laser scattering particle size analysis (Model: Malvern Zetasizer 1000, Worcestershire, UK). The particle size distribution of $BaO–SiO_2$ glass with different milling times is shown in Fig. 1. The mean diameter, D50, of the ground glass frit was 185, 326, 499 and 1200 nm and the corresponding milling times were 5, 3, 2 and 0.5 h.

### 2.2. Sample preparation

$Ba(Ti_{0.82}Zr_{0.18})O_3$ (BTZ) ceramics with a mean particle size of about 0.5 μm were fabricated by a conventional solid state method. The BTZ powders were mixed with 0.5 mol% reagent-grade $Mn_3O_4$ and different particle sizes of $BaO–SiO_2$ glass 0.3 wt%. The mixture was homogenized with alcohol in a ball mill for 24 h. To prepare the powders for pressing, they were

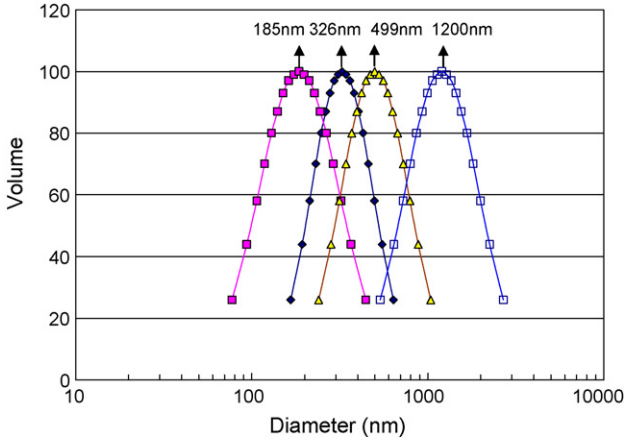


Fig. 1. The particle size distribution of $BaO–SiO_2$ glass measured by laser scattering with different milling times.

mixed with 3 wt% of 15% PVA solution, dried, pulverized using a mortar, and then sieved through a 120 mesh screen. After further drying at 100 °C, the mixtures were uniaxially pressed into discs 12 mm in diameter and 2 mm in thickness under 100 MPa. Sintering was conducted at 1275 °C for 3 h in a reduction atmosphere. The oxygen partial pressure was controlled by the mixture of nitrogen and hydrogen saturated with $H_2O$ at 50 °C and continuously monitored using a zirconia cell at 800 °C. The measured values of oxygen partial pressure corresponded to $2 \times 10^{-5}$ Pa at 1275 °C. Reoxidation of the ceramic specimens was carried out at 900 °C for 2 h in a nitrogen atmosphere.

### 2.3. Evaluation of the dielectric characteristics

The density of the sintered composites was measured by the Archimedes method, with all the specimens showing more than 99% theoretical density. The free surface of the sintered ceramic discs was observed using a scanning electron microscope (SEM; Model: JSM-5600, JEOL Ltd., Japan) with an accelerating voltage of 25 kV, and the mean grain size was calculated according to the line intercept method.

Copper electrodes were attached to the surface of the sintered discs and fired at 900 °C for 10 min to measure the dielectric properties. Dielectric permittivity and the dissipation factor of the disc type capacitor were measured using an impedance analyzer (Model: HP4284A, Agilent Tech., CA, USA). For each type of sample, permittivity measurements were carried out by averaging the data for a least five specimens. The measurements were carried out in a temperature range of −55 to 125 °C at 1 kHz and 1 $V_{rms}$. Isolation resistance (IR) was measured using a high resistance meter (Model: HP4339B, Agilent Tech., CA, USA) at room temperature. A thermal mechanical analyzer (TMA; Model: Setsys Evolution 18, Setaram, France) was used to determine the shrinkage of the samples fired in a reductive atmosphere of 0.5% $H_2$ + 99.5% $N_2$ with a heating rate of 5 °C/min.

The crystal structure of the samples was identified using an X-ray diffractometer (XRD; Model D-MAX IIIv, Rigaku Co., Tokyo, Japan), in conjunction with Cu Kα radiation, operated at 30 kV, 20 mA, and a scanning rate of $1^\circ\,min^{-1}$ within the range of $2\theta$ from 20° to 80°. The microstructure of the samples was examined with a transmission electron microscope (TEM; Model: JEM-3010, JEOL Ltd., Japan) equipped with an energy-dispersive X-ray spectroscope (EDS). TEM samples were prepared using the Focused Ion Beam (FIB; Model: SMI 3050, SII NanoTech. Inc., Tokyo, Japan) approach.

## 3. Results and discussion

The densities of the sintered samples measured by the Archimedes method were 6.014, 6.006, 5.991 and 6.079 g/cm$^3$ when the glass particle size was increased from 185, 326, 499 to 1200 nm, respectively. More than 99% of the theoretical density was achieved for all sintered samples. The sintering temperature of Mn-doped BTZ ceramics could be reduced effectively to 1275 °C by doping them with 0.3 wt% of BaO–$SiO_2$ glass. The densification of BTZ ceramics was enhanced by liquid phase sintering at lower temperature. Moreover, the specimen with 185 nm glass had a lower linear shrinkage ratio of 17.44% after firing in a reductive atmosphere, compared to that of 19.18% for the specimen with 1200 nm glass. This is due to the higher green packing density with finer glass frit, and the green density of the specimen with 185 nm glass was 3.72 g/cm$^3$, which was higher than the 3.66 g/cm$^3$ for the specimen with 1200 nm glass. The

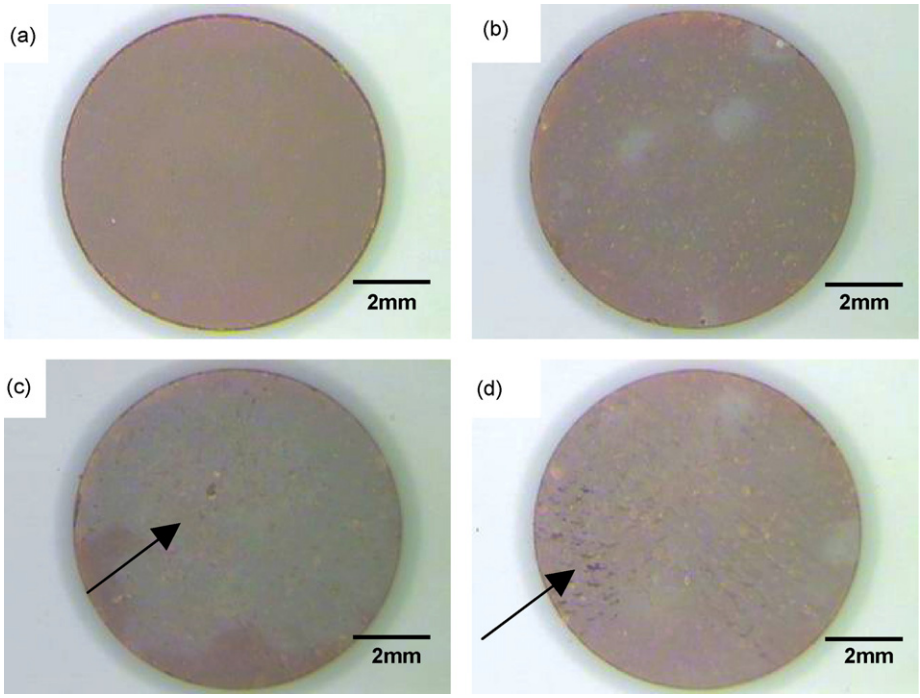


Fig. 2. The metallographic photographs of the sintered samples doped with various D50 BaO–$SiO_2$ glass: (a) D50 = 185 nm, (b) D50 = 326 nm, (c) D50 = 499 nm, and (d) D50 = 1200 nm. More than 99% of theoretical density was achieved for all samples.

sample size for the green density measurement was 10 pieces per sample. The lower shrinkage ratio was beneficial to reducing the inner stress during the ceramic–metal co-firing procedure. Fig. 2 shows the metallographic images of the sintered samples doped with various glass particle sizes of $BaO–SiO_2$. From this figure, it is seen that surface porosity gradually increased along with the glass particle size, as indicated by the arrows in Fig. 2(c) and (d). This porosity may be harmful to the dielectric properties of the material, such as isolation resistance and humidity endurance. Specimens with 185 nm glass frit were shown to be free of pores, and also had the most homogeneous structure and the least color difference on the surface of the sintered discs, as shown in Fig. 2(a). This might be because the finer glass frit is more reactive and dispersive in the ceramics. These results are consistent with those in Al-Allak et al.'s study,[14] which found that the eutectic temperature of $BaTiO_3$ ceramic decreased from approximately 1320 to 1260 °C after the addition of $SiO_2$. In the current work, the dispersion of dopants in the material and microstructure uniformity was promoted by the presence of silica and the more homogeneous, finer glass. It is assumed that better uniformity reduces the amount of glass usage and prevents the degradation of dielectric properties due to the dilution of low *K* additives.

Fig. 3 shows the XRD patterns of the BTZ-based specimens as a function of the glass particle size. For samples containing glass frit with a D50 from 185 to 1200 nm, only a single perovskite Ba(Ti, Zr)$O_3$ phase was observed. Except for the diffracted reflection from the silicon standard, no second phase was observed. This suggests that the $BaO–SiO_2$ glass was completely incorporated into the $ABO_3$ lattice to make a solid solution. The separation of the (0 0 2) and (2 0 0) reflections is

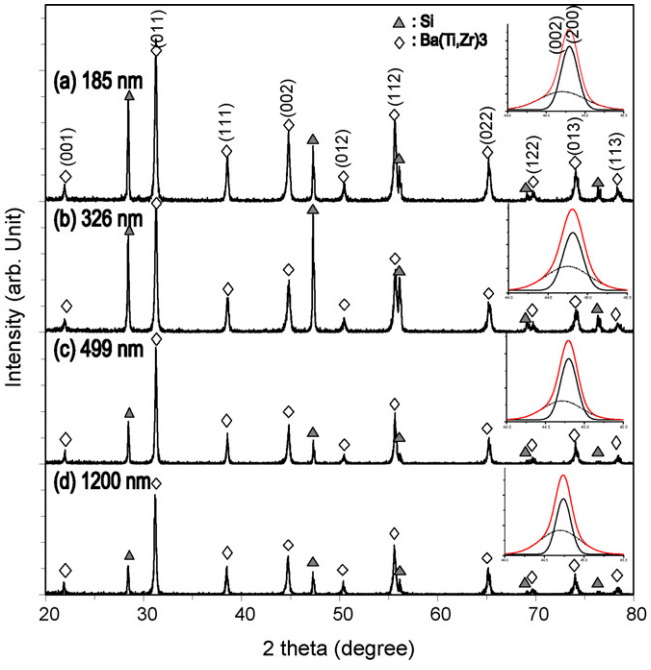


Fig. 3. XRD patterns of the Mn-doped BTZ specimens as a function of the glass particle size: (a) D50 = 185 nm, (b) D50 = 326 nm, (c) D50 = 499 nm, and (d) D50 = 1200 nm.

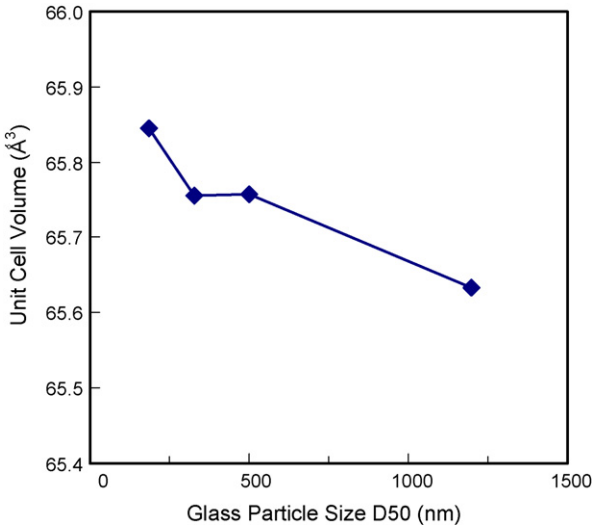


Fig. 4. Changes in unit cell volume of the Mn-doped BTZ specimens as a function of the glass particle size.

not obvious, which indicates that the Mn-doped Ba(Ti, Zr)$O_3$ exhibits a pseudo-cubic structure. To quantify the change in the degree of tetragonality, the integrated (0 0 2) and (2 0 0) peaks were enlarged and resolved.[19] Each measured diffraction curve was fitted to two Gaussian curves which correspond to the (0 0 2) and (2 0 0) peaks using Origin 8 software (Origin Lab Corp., MA, USA), and the results are shown in Fig. 3. When the tetragonality and cubic phases coexist, the (0 0 2) peak is only from tetragonal phase but the (2 0 0) peak is from both the tetragonal and cubic phases. Therefore, the ratio of the intensity of the two peaks, $I_{002}/I_{200}$, indicates the volume ratio of the tetragonal phase. According to Fig. 3(b) and (a), the $I_{002}/I_{200}$ ratio decreases from 40.8% to 30.2% when the glass particle size falls from 326 to 185 nm. This demonstrates that the volume of the tetragonal phase decreases and the cubic phase increases with glass that is 185 nm or finer. Kuromitsu et al.[15] reported that a $Ba_2SiO_4$ and $Ba_2TiSiO_8$ compound was observed in the $PbO–SiO_2$ glass system, and that this inhibits the grain growth. However, neither of these substances was found in the study, which may be due to the amount of glass frit that was added. The effects of the glass particle size on the unit cell volume of the Mn-doped BTZ specimens estimated from Fig. 3 are shown in Fig. 4. The unit cell volumes of the samples' perovskite phases were determined using the traditional method of indexing and calculation with the Least-squares Powder Diffraction Program, UnitCell, written by Holland and Redfern,[22] in which silicon was used as the internal standard. When the glass particle size was decreased, the volume of the samples' unit cell became larger. The expansion in the unit cell volume induced by the finer glass was due to the more homogeneous distribution of glass, which enhances the occupation of $Mn^{2+}$ (0.83 Å) ions in the $Ti^{4+}$ (0.6 Å) and $Zr^{4+}$ (0.72 Å) site of the perovskite structure. The results agree with those in Chen et al.,[23] which found that the formation of a liquid phase enhances the cation diffusion via dissolution and reprecipitation processes in the sintering process of $BaTiO_3$ with excess $SiO_2$.

SEM micrographs of the sintered disc surfaces with various glass particle sizes are shown in Fig. 5. The mean grain size of

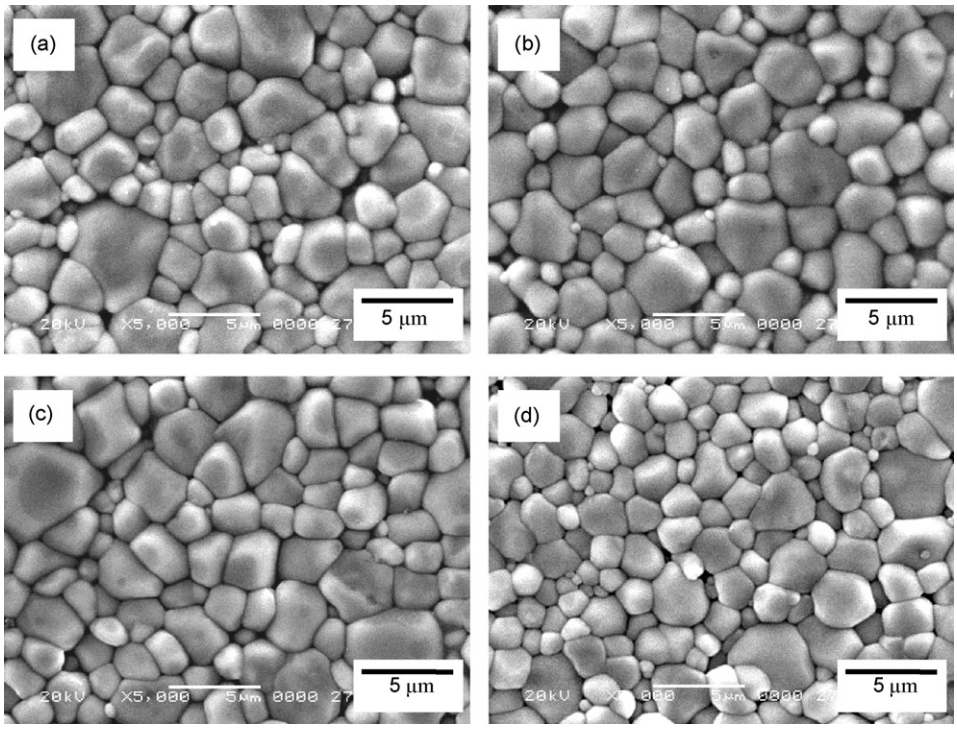


Fig. 5. SEM micrographs of the sintered samples with various glass particle sizes: (a) D50 = 185 nm, (b) D50 = 326 nm, (c) D50 = 499 nm, and (d) D50 = 1200 nm.

Mn-doped BTZ ceramics sintered at 1275 °C for 3 h as a function of glass particle size is shown in Fig. 6. The mean grain size was calculated according to the line intercept method from scanning electron microscopy. The grain size decreased with the increasing particle size of the glass frit, as the finer glass penetrates and wets the ceramic interface more effectively and enhances the grain growth. The average grain size of the samples increased from 2.02 to 2.60 μm when the glass particle size was decreased from 1200 to 185 nm. The presence of more dispersive liquid phase enhanced the dissolution of the $Mn^{2+}$ ions which occupied the B-sites of Ba(Ti, Zr)$O_3$ and decreased the A/B ratio, and hence liquid eutectic Ba(Ti, Zr)$O_3$–$Ba_6$(Ti, Zr)$_{17}O_{40}$ was induced, and this enhanced the grain growth.[24] In other words, liquid phase sintering becomes more efficient when using glass frit with a finer particle size. The substitution of $Mn^{2+}$ into Ba(Ti, Zr)$O_3$, which was enhanced by liquid phase sintering, seems to be closely related to the grain growth of BTZ ceramics. Moreover, it can be seen that the grain size in Fig. 5 is much larger than the initial BTZ ceramics, which reveals the solution reprecipitation process during the sintering of the BTZ ceramics. This indicates the importance of the homogeneous distribution of the liquid phase with the doping of $Mn^{2+}$ into the BTZ ceramics. The wettability of the finer glass is higher, and thus the fluctuation of glass in specimens with finer glass may be relatively low. The wettability of the liquid phase provides the excessive dissolution of dopant, which might increase the dopant transportability to the BTZ grains and lead to the homogenization of the dopant concentration. These results support those in Zubair and Leach's study,[16] which found that the addition of $SiO_2$ and Mn may assist the homogenization of the microstructure during sintering through the formation of a liquid phase. However, except for the corresponding changes in lattice parameters, we were unable to confirm this from TEM/EDS compositional analysis, due to the low concentration of the additives.

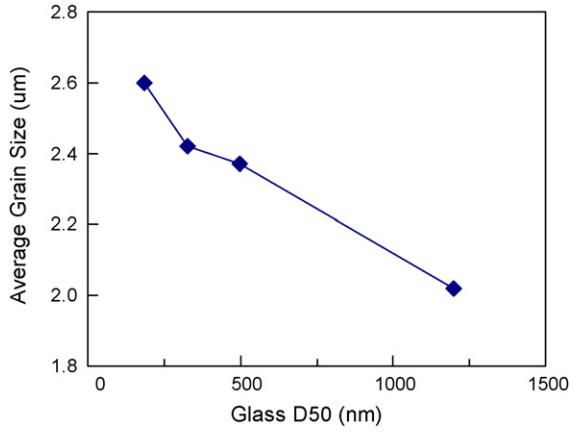


Fig. 6. The mean grain size of Mn-doped BTZ ceramics sintered at 1275 °C for 3 h as a function of glass particle size.

Fig. 7 shows TEM micrographs of the sintered samples with various glass particle sizes, and small dark grains can be seen in the grain boundaries with finer glass additives, indicated by point A in Fig. 7(a). The corresponding selected area diffraction pattern (SADP) was obtained, and this reveals that the crystal structure of the small dark grain (labeled A) is perovskite with a zone axis $Z = [1\,1\,0]$. Furthermore, the diffraction pattern of the large grain (labeled C) in Fig. 7(c) is evidence of the crystalline Ba(Ti, Zr)$O_3$ phase with pseudo-cubic symmetry. The composition of different regions analyzed using an energy-dispersive X-ray spectrometer (EDS) is listed in Table 1. The dark grains present in the triple junction of the specimen, indicated as point A in Fig. 7(a), were identified as the relatively

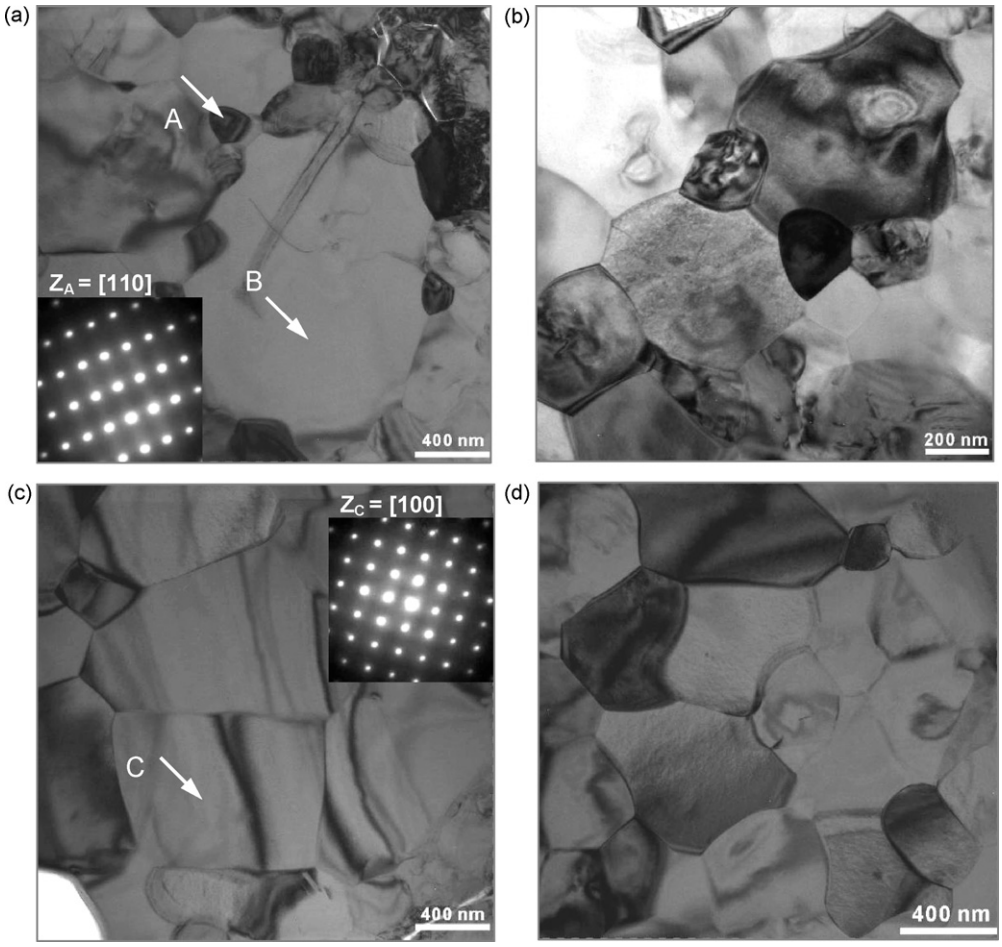


Fig. 7. Bright-field TEM micrographs of microstructure with various glass particle sizes: (a) D50 = 185 nm, (b) D50 = 326 nm, (c) D50 = 499 nm, and (d) D50 = 1200 nm.

silicon-rich Ba(Ti, Zr)$O_3$ phase, in which the atomic ratio of Si is 1.29%, as compared with 0.29% for point B in Fig. 7(a) and 0.42% for point C in Fig. 7(c). This finding is in good agreement with the XRD results in Fig. 3. No second phase was detected, except for the solid solution with a single perovskite structure, since the silicon-rich phase exhibited as really dark grains have the same perovskite structure and it is possible that there is a residual glass phase (not shown here) that is amorphous. The appearance of the silicon-rich phase in the triple junction and at the grain boundaries demonstrates that the grain growth in the samples is enhanced by the formation of a liquid phase. Moreover, the dark grains reveal a more homogeneous distribution with decreasing glass particle size. This indicates that homogenization of the silicon-rich Ba(Ti, Zr)$O_3$ phase is enhanced by reducing the glass particle size.

Table 1
The composition of different regions as indicated as points A, B and C in Fig. 7 analyzed using an energy-dispersive X-ray spectrometer (EDS) in TEM.

| Atom% | O (K) | Si (K) | Ba (L) | Ti (K) | Zr (L) | Mn (K) |
|---|---|---|---|---|---|---|
| Point A | 57.03 | 1.29 | 21.90 | 15.89 | 3.86 | <0.1 |
| Point B | 58.39 | 0.29 | 21.33 | 16.26 | 3.95 | <0.1 |
| Point C | 57.74 | 0.42 | 21.59 | 16.35 | 3.88 | <0.1 |

Fig. 8 shows the permittivity and the dissipation factor (D.F.) of Mn-doped BTZ specimens as a function of the glass particle size at room temperature. The specimens with 185 and 326 nm glass exhibit higher permittivity than those with 499 and 1200 nm particles. Kell and Hellicar[5] and Hansen et al.[6] mentioned that the broad dielectric maxima rises with increasing

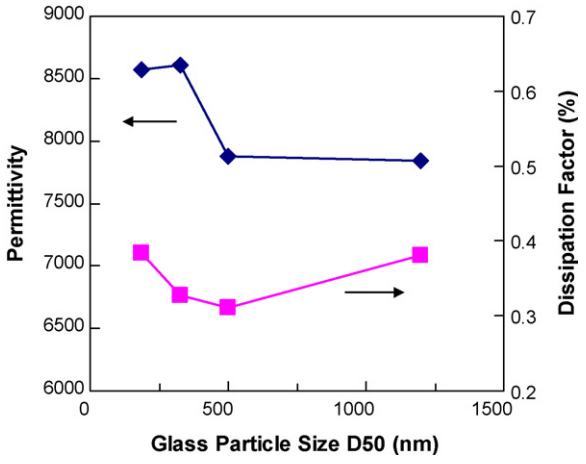


Fig. 8. Permittivity and the dissipation factor (D.F.) of Mn-doped BTZ specimens as a function of the glass particle size at room temperature.

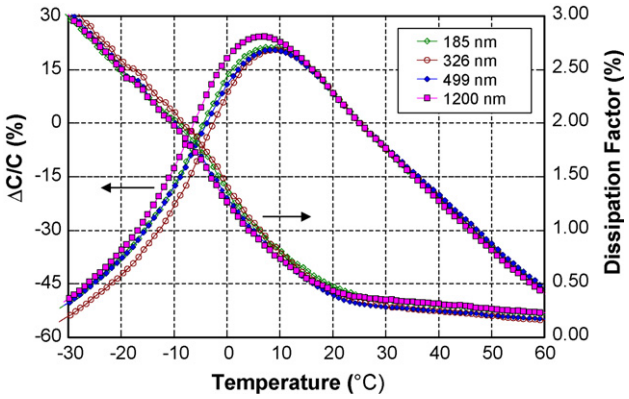


Fig. 9. Temperature coefficient of capacitance (TCC) and dissipation factor (D.F.) of Mn-doped BTZ specimens with different glass particle sizes added.

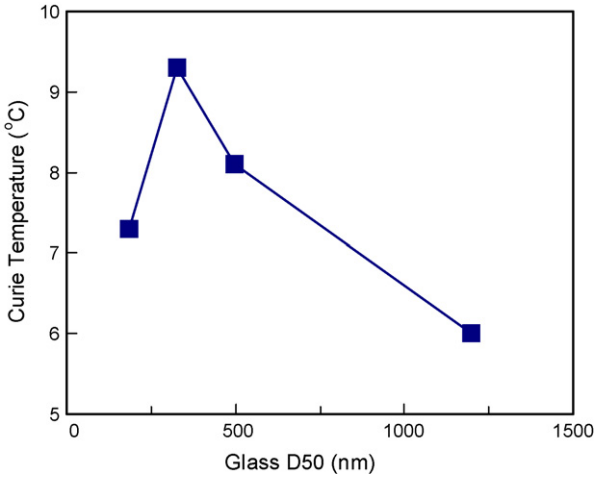


Fig. 10. The Curie temperature of Mn-doped BTZ specimens as a function of the glass particle size.

grain size. However, the average grain size of the samples under the same sintering conditions increased with the decreasing particle size of the glass frit, as shown in Fig. 6. Thus, the relation between permittivity and grain size is not clear. It is assumed that the permittivity at room temperature was not only influenced by the grain size difference, but also by the Curie temperature variation induced by the distribution of incorporated atoms. Moreover, the dissipation factor (D.F.) decreased from 0.380 to 0.311 when the glass particle size was decreased from 1200 to 499 nm. It is assumed that the conduction electrons were trapped by the acceptors $Mn^{2+}$, which were encouraged to dissolve in the grains by the decreasing particle size of the glass additives. The composition change in the grain boundary eliminates the leakage current and reduces the dissipation factor. In addition, the inhomogeneities in the specimens with 1200 nm glass, as shown in Fig. 2(d), also have a harmful effect on leakage current. When the glass size decreased from 499 to 185 nm, the dissipation factor increased from 0.311 to 0.384. In Fig. 6, it is seen that the grain size increase dominates the amount of leakage current and leads to a rise in D.F. It has been reported that motion of the 90° domain walls is one of the sources of dielectric loss.[25] In addition, it has been shown that limiting domain wall motion by the pinning effect of the grain boundaries decreases with increasing grain size, and raises the amount of leakage current.[26]

Fig. 9 shows the temperature coefficient of capacitance (TCC) and the D.F. for Mn-doped BTZ ceramics doped with different size glass particles. The Curie temperature of Mn-doped BTZ specimens as a function of the glass particle size is shown in Fig. 10. When the glass particle size decreased from 1200 to 326 nm, the Curie temperature shifted from 6.0 to 9.3 °C. In Fig. 4 it can be seen that the expansion of the BTZ lattice by $Mn^{2+}$ incorporation with decreasing particle size from 1200 to 326 nm may hinder the phase transition, since the lattice volume of BTZ decreases through a transition from the tetragonal to cubic phase, which leads to an increasing Curie temperature. This is because the extent of the incorporation between the ceramic and the distribution of incorporated atoms alters the Curie temperature significantly. When the glass particle size was further decreased to 185 nm, the Curie temperature declined significantly, from 9.3 to 7.3 °C. From Figs. 5 and 6, it can be seen that the grain size was increased from 2.42 to 2.60 μm when the glass particle size was decreased from 326 to 185 nm. A more homogeneous glass distribution enhances the grain growth, and leads to faster mass transport of dopants such as $Mn^{2+}$ and the formation of a more homogeneous grain structure. The internal stress inside the grain structure decreases significantly with a coarser grain size, and promotes the transition from the tetragonal to cubic phases, as shown in Fig. 3(a) and (b), which leads to the drop in Curie temperature. The observed drop of Curie temperature with decreasing glass particle size from 326 to 185 nm may be also attributed to $Zr^{4+}$ ions from the yttria stabilized zirconia (YSZ) media, since the milling time for these sizes is longer and it can be assumed that wear loss is proportional to milling time. As Kell and Hellicar[5] indicated, the substitution of $Ti^{4+}$ ions by $Zr^{4+}$ ions leads to a reduction in Curie temperature for $BaTiO_3$-based ceramics. The Curie point is thus shifted towards lower temperatures under the combined effects of a more homogeneous grain structure and the contamination of $Zr^{4+}$ ions induced by wear to the YSZ balls. Moreover, the contamination with $Zr^{4+}$ ions may alter the surface tension of the liquid, which thereby prefers to be located in the triple junction of every grain, which would also ensure greater homogenization. It is also possible that the shift of the Curie point towards a higher temperature may be attributed to $Y^{3+}$ ions from the YSZ media. However, the influence is relatively small and thus ignored due to the relatively low yttrium concentration in the YSZ media.

The role of glass is not limited to its use as a sintering aid, but also extended to control the grain growth and dopant transportability, which modify the dielectric properties of ceramics. The influence of glass particle size on the compositional distribution of Mn-doped BTZ ceramics is obvious, and the microstructure and electrical properties are changed accordingly. In practice, the amount of glass addition could be minimized to reduce the negative side effects, since more homogeneous glass distribution works is more efficient with regard to densification. It is assumed in this work that the homogenization of glass and dopant concentration controlled by the particle size of the glass frit can play an important role in the development of novel multilayer ceramic capacitors with ultra-thin dielectric layers.

## 4. Conclusions

1. It is found that finer $BaO–SiO_2$ glass frit doped ceramics have a more homogeneous structure and the mean grain size decreases as the particle size of the glass frit increases. A finer and better spreading glass phase penetrates the BTZ ceramic interface more easily and enhances the grain growth.
2. The expansion of the unit cell volume induced by the finer glass is due to the homogeneous distribution of glass, which enhances the occupation of $Mn^{2+}$ ions in the perovskite structure and results in the increased grain growth.
3. The extent of the $Mn^{2+}$ incorporation in BTZ ceramic increases with decreasing glass particle size, from 1200 to 326 nm, and shifts the Curie temperature. When the glass particle size is further reduced to 185 nm, the Curie temperature declines significantly due to the combined effect of a more homogeneous grain structure with lower tetragonality, and the contamination of $Zr^{4+}$ ions induced by wearing of the milling balls.
4. Microstructural evaluation by transmission electron microscopy (TEM) indicates that glass particle size has a dramatic influence on the sintering behavior, microstructure and dielectric characteristics of Mn-doped BTZ ceramics. It is considered that glass homogenization controlled by the particle size of glass frit will have an important role in the development of novel multilayer ceramic capacitors with ultra-thin dielectric layers.

## Acknowledgement

The authors would like to thank the Darfon Electronics Corp. for their financial and technical support.

## References

1. Kishi H, Mizuno Y, Chozono H. Base-metal electrode-multilayer ceramic capacitors: past, present and future perspectives. *Jpn J Appl Phys* 2003;**42**:1–15.
2. Mizuno Y, Hagiwara T, Kishi H. Microstructural design of dielectrics for Ni-MLCC with ultra-thin active layers. *J Ceram Soc Jpn* 2007;**115**:360–4.
3. Waser R, Balatu T, Härdtl K. DC electrical degradation of perovskite-type titanates. I: ceramics. *J Am Ceram Soc* 1990;**73**:1645–53.
4. Chazono H, Kishi H. Dc-electrical degradation of the BT-based material for multilayer ceramic capacitor with Ni internal electrode: impedance analysis and microstructure. *Jpn J Appl Phys* 2001;**40**:5624–9.
5. Kell RC, Hellicar NJ. Structure transitions in barium titanate zirconate transducer materials. *Acustica* 1956;**6**:235–8.
6. Hansen P, Hennings D, Schreinemacher H. Dielectric properties of acceptor-doped $(Ba,Ca)(Ti,Zr)O_3$ ceramics. *J Electroceram* 1998;**2**:85–94.
7. Weber U, Greuel G, Boettger U, Weber S, Hennings D, Waser R. Dielectric properties of $Ba(Zr,Ti)O_3$-based ferroelectrics for capacitor applications. *J Am Ceram Soc* 2001;**84**:759–66.
8. Wang CH. Microstructure and characteristics of $Ba(Ti,Zr)O_3$ ceramics with addition of glass frit. *Jpn J Appl Phys* 2002;**41**:5317–22.
9. Morita K, Mizuno Y, Chazono H, Kishi H. Effect of Mn addition on dc-electrical degradation of multilayer ceramic capacitor with Ni internal electrode. *Jpn J Appl Phys* 2002;**41**:6957–61.
10. Nakano Y, Sato A, Hitomi A, Nomura T. Microstructure and related phenomena of multilayer ceramic capacitors with Ni-electrode. *Ceram Trans* 1993;**32**:119–28.
11. Wang CH, Wu L. $Ba(Ti, Zr)O_3$ ceramics sintered with lead borate glass. *Jpn J Appl Phys* 1993;**32**:3518–25.
12. Wang SF, Yang TCK, Wang YR, Kuromitsu Y. Effect of glass composition on the densification and dielectric properties of $BaTiO_3$ ceramics. *Ceram Int* 2001:157–62.
13. Hennings DFK, Janssen R, Reynen PJL. Control of liquid-phase-enhanced discontinuous grain growth in barium titanate. *J Am Ceram Soc* 1987;**70**:23–7.
14. Al-Allak HM, Parry TV, Russell GJ, Woods J. Effects of aluminium on the electrical and mechanical properties of PTCR $BaTiO_3$ ceramics as a function of the sintering temperature. *J Mater Sci* 1988;**23**:1083–9.
15. Kuromitsu Y, Wang SF, Yoshikawa S, Newnham RE. Interaction between barium titanate and binary glasses. *J Am Ceram Soc* 1994;**77**:493–8.
16. Zubair MA, Leach C. The influence of cooling rate and $SiO_2$ additions on the grain boundary structure of Mn-doped PTC thermistors. *J Eur Ceram Soc* 2008;**28**:1845–55.
17. Liu G, Roseman RD. Effect of BaO and $SiO_2$ addition on PTCR $BaTiO_3$ ceramics. *J Mater Sci* 1999;**34**:4439–45.
18. Hsiang HI, Hsi CS, Huang CC, Fu SL. Low temperature sintering and dielectric properties of $BaTiO_3$ with glass addition. *Mater Chem Phys* 2009;**113**:658–63.
19. Bae ST, Lee S, Kim JH, Hong KS, Shin H, Jung HS. Effect of glass composition on the dielectric properties of a liquid-phase-sintered MgO-doped $BaTiO_3$. *J Am Ceram Soc* 2008;**91**:2205–10.
20. Jeon HP, Lee SK, Kim SW, Choi DK. Effects of $BaO–B_2O_3–SiO_2$ glass additive on densification and dielectric properties of $BaTiO_3$ ceramics. *Mater Chem Phys* 2005;**94**:185–9.
21. Zhang B, Yao X, Zhang L. Study on the structure and dielectric properties of $BaO–SiO_2–B_2O_3$ glass-doped $(Ba,Sr)TiO_3$ ceramics. *Ceram Int* 2004;**30**:1767–71.
22. Holland TJB, Redfern SAT. Unit cell refinement from powder diffraction data; the use of regression diagnostics. *Mineralog Mag* 1997;**61**:65–77.
23. Chen JY, Jin W, Yao Y. Study of the anomalous grain growth of $BaTiO_3$ ceramics. *Ferroelectrics* 1993;**142**:153–9.
24. Jain TA, Fung KZ, Chan J. Effect of the A/B ratio on the microstructures and electrical properties of $(Ba_{0.95\pm x}Ca_{0.05})(Ti_{0.82}Zr_{0.18})O_3$ for multilayer ceramic capacitors with nickel electrodes. *J Alloys Compd* 2009;**468**:370–4.
25. McNeal MP, Jang SJ, Newnham RE. Particle size dependent frequency dielectric properties of barium titanate. *J Appl Phys* 1996;**83**:837–40.
26. Zhang L, Zhong WL, Wang CL, Peng YP, Wang YG. Size dependence of dielectric properties and structural metastability in ferroelectrics. *Eur Phys J B* 1999;**11**:565–73.